Supplement of Biogeosciences, 15, 2021–2032, 2018
https://doi.org/10.5194/bg-15-2021-2018-supplement

Biogeosciences Open Access EGU

Supplement of

High-frequency productivity estimates for a lake from free-water CO_2 concentration measurements

Maria Provenzale et al.

Correspondence to: Maria Provenzale (maria.provenzale@helsinki.fi)

Contents of this file

1. Section S1: introduction
2. Section S2: calculation of the eddy covariance CO_2 flux
3. Section S3: Smith (1936) and Jassby and Platt (1976) model equations
4. Figg. S1-S14
5. Table S1: Michaelis-Menten, Smith and Jassby and Platt model fit statistics

S1 Introduction

This supporting information provides details on how the flux between Lake Kuivajärvi and the atmosphere, measured by eddy covariance, was calculated (Sect. S2). It also provides additional figures (Figg. S1-S14). Figures S1 and S2 consist of maps, showing the location of Lake Kuivajärvi in Finland, its bathymetry and the position of the measuring raft. Figure S3 is a schematic representation of the measuring system we built for the CO_2 concentration in the water. Figure S4 displays the time series of isotherms of the lake for the whole summers, while Figg. S5-S14 display the time series of isotherms, of the Schimdt stability and of the CO_2 concentration at 0.2 m for the periods of stable stratification chosen for analysis.

S2 Calculation of the eddy covariance fluxes

The CO_2 flux between the lake and the atmosphere was measured using the eddy covariance (EC) technique (Aubinet *et al.*, 2012). The fluxes were calculated as in Vesala et al. (2006); Mammarella et al. (2009, 2015). The chosen averaging time was 30 minutes, and the mean values were obtained by block-averaging. Before calculating the covariances, the data were despiked according to standard methods (Vickers and Mahrt , 1997). Successively, the coordinate system was rotated via a two-step rotation (Kaimal and Finnigan, 1994), so that the x axis was parallel to the mean wind direction and the mean of the vertical wind velocity was 0. The CO_2 mole fraction values were converted to dry mole fraction values (Burba *et al.*, 2012). The time lag between the measurement of the vertical wind velocity and the measurement of the CO_2 mole fraction was determined for each 30-min interval separately, by maximizing the difference between their cross-correlation function and the line connecting the values of the cross-correlation at the lag window boundaries (Clement , 2004). The fluxes were also corrected for high-frequency and low-frequency losses, according to Foken *et al.* (2012).

Finally, the fluxes were quality screened. Data from 30-min intervals when the prevailing wind direction was not along the lake were discarded. Furthermore, data were also discarded when the absolute value of skewness of the CO_2 concentration or of the vertical wind velocity was > 2 and the kurtosis was < 1 or > 8 (Vickers and Mahrt , 1997). The flux steady-state test (FST) was also applied (Foken and Wichura, 1996), and data were rejected when $\mathrm{FST} > 0.3$. The CO_2 storage flux in the air between the water surface and the height of the measuring system (1.5 m) is negligible.

S3 Smith and Jassby and Platt model equations and fit results

We checked whether the Smith (1936) or the Jassby and Platt (1976) models were a better fit to the data than the Michaelis-Menten curve. Maintaining the assumption that the daytime respiration rate equals the nighttime respiration rate and that they depend exponentially on temperature (Carignan et al., 2000), we still had:

$$NPP = GPP - R_{\mathrm{h}} = GPP - r_0\, Q_{10}^{T/10}, \tag{S1}$$

with T as the water temperature (in °C), Q_{10} as a non-dimensional temperature coefficient with a value of 2 for freshwater communities, and r_0 as the parameter representing the basal respiration of phytoplankton ($\mu\mathrm{mol}(\mathrm{CO_2})\,\mathrm{m}^{-2}\,\mathrm{s}^{-1}$). GPP was

expressed as

$$GPP = \frac{p_{\max}\,\alpha\,PAR}{\sqrt{p_{\max}^2 + \alpha^2\,PAR^2}} \tag{S2}$$

following Smith (1936), and as

$$GPP = p_{\max}\,\tanh\frac{\alpha\,PAR}{p_{\max}} \tag{S3}$$

following Jassby and Platt (1976), with $p_{\max}$ as the maximum potential photosynthetic rate ($\mu\mathrm{mol}(\mathrm{CO_2})\,\mathrm{m^{-2}\,s^{-1}}$) and α as the curve slope at low light levels ($\mu\mathrm{mol}(\mathrm{CO_2})\,\mathrm{m^{-2}\,s^{-1}}\,\left(\mu\mathrm{mol}(\mathrm{ph})\,\mathrm{m^{-2}\,s^{-1}}\right)^{-1}$).

The fit statics are reported in Table S1 (the Michaelis-Menten fit statistics are also reported, for comparison). They show that there is a good agreement between all the models and the data, and that there is no significant reason to discard the Michaelis-Menten curve.

References

Aubinet, M., Vesala, T., and Papale, D.: Eddy Covariance: A Practical Guide to Measurement and Data Analysis, Springer, Dordrecht, the Netherlands, 2012.

Burba, G., et al.: Calculating CO_2 and H_2O eddy covariance fluxes from an enclosed gas analyzer using an instantaneous mixing ratio, Global Change Biol., 18, 385-399, 2012.

Carignan, R., Planas, D., Vis, C.: Planktonic production and respiration in oligotrophic Shield lakes, Limnol. Oceanogr., 45, 189-199, 2000.

Clement, R.: Mass and energy exchange of a plantation forest in Scotland using micrometeorological methods, Ph.D. thesis, Univ. of Edinburgh, Edinburgh, UK, 2004.

Foken, T., and Wichura, B.: Tools for quality assessment of surface-based flux measurements, Agric. For. Meteorol., 78, 83-105, 1996.

Foken, T., Aubinet, M., and Leuning, R.: The eddy covariance method, pp 1-19, In Aubinet, M., and others [eds.], Eddy Covariance: A Practical Guide to Measurement and Data Analysis, Springer, Dordrecht, the Netherlands, 2012.

Jassby, A. D., and Platt, T.: Mathematical formulation of the relationship between photosynthesis and light for phytoplankton, Limnol. Oceanogr., 21, 540-547, 1976.

Kaimal, J. C., and Finnigan, J. J.: Atmospheric Boundary Layer Flows, Their Structure and Measurements, Oxford Univ. Press, New York, 1994.

Mammarella, I., Launiainen, S., Grönholm, T., Keronen, P., Pumpanen, J., Rannik, Ü., and Vesala, T.: Relative humidity effect on the high-frequency attenuation of water vapor flux measured by a closed-path eddy covariance system, J. Atmos. Ocean. Technol., 26, 1856-1866, 2009.

Mammarella, I., Nordbo, A., Rannik, Ü, and others: Carbon dioxide and energy fluxes over a small boreal lake in Southern Finland, J. Geophys. Res. Biogeosci., 120, 1296-1314, 2015.

Smith, E. L.: Photosynthesis in relation to light and carbon dioxide, Proceedings of the National Academy of Sciences, 22, 504-511, 1936.

Vesala, T., Huotari, J., Rannik, Ü., Suni, T., Smolander, S., Sogachev, A., Launiainen, S., and Ojala, A.: Eddy covariance measurements of carbon exchange and latent and sensible heat fluxes over a boreal lake for a full open-water period, J. Geophys. Res., 111, D11101, 2006.

Vickers, D., and Mahrt, L.: Quality control and flux sampling problems for tower and aircraft data, J. Atmos. Oceanic Technol., 14, 512-526, 1997.

Figure S1. The location of Lake Kuivajärvi in Finland, represented by the red "x". Its coordinates are 61°50.743' N, 24°17.134' E. This figure contains data from the National Land Survey of Finland Topographic Database 12/2015.

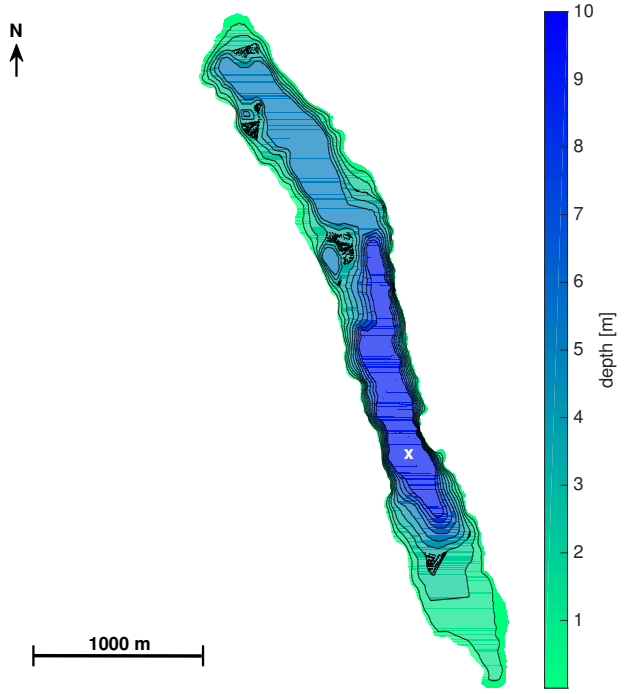

Figure S2. The bathymetry of Lake Kuivajärvi. The position of the raft with the measuring instruments is marked in the picture with a white "x".

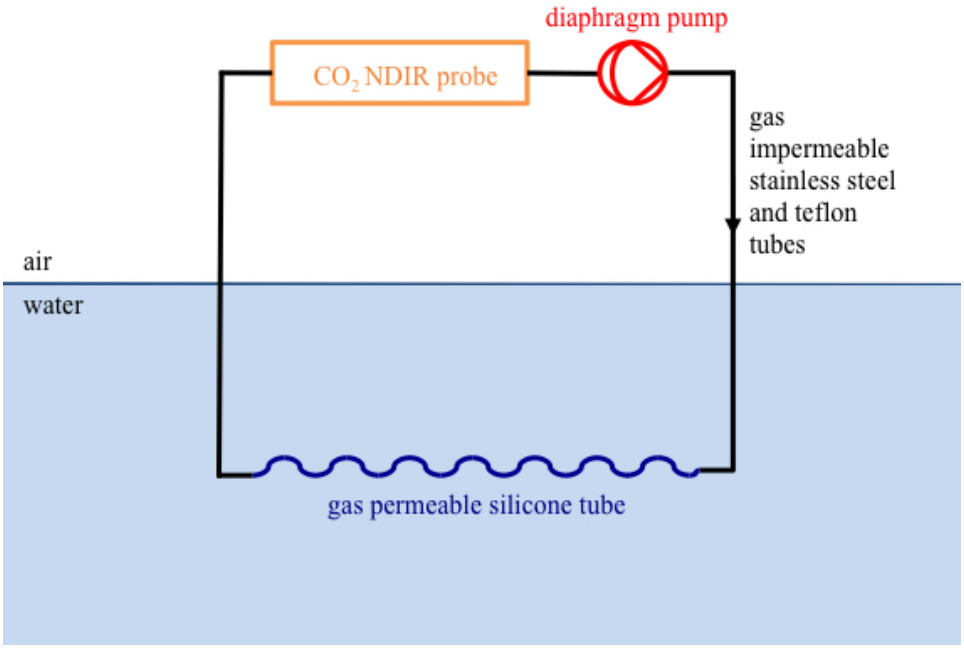

Figure S3. The measuring system, consisting in the CO_2 NDIR probe (CARBOCAP® GMP343, Vaisala Oyj, Vantaa, Finland) for the CO_2 concentration in the air, gas impermeable stainless steel and teflon tubes, a submerged silicone gas permeable tube (Rotilabo 9572.1, Carl Roth GmbH and Co. KG, Karlsruhe, Germany) and a diaphragm pump to circulate the air in the system (KNF Neuberger Micro gas pump, KNF Neuberger AB, Stockholm, Sweden).

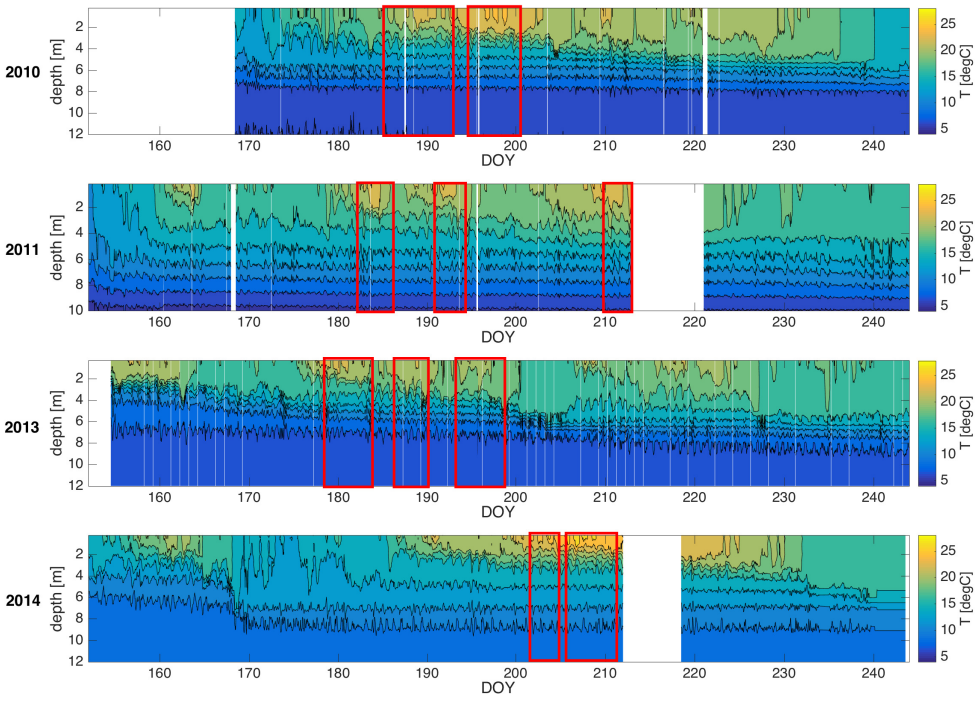

Figure S4. The temperature maps of the lake for the studied summers, from 1 June (DOY = 152) to 31 August (DOY = 243). The red rectangles indicate the periods of stable stratification that were chosen for the data analysis. All of them are between mid-June and the end of July.

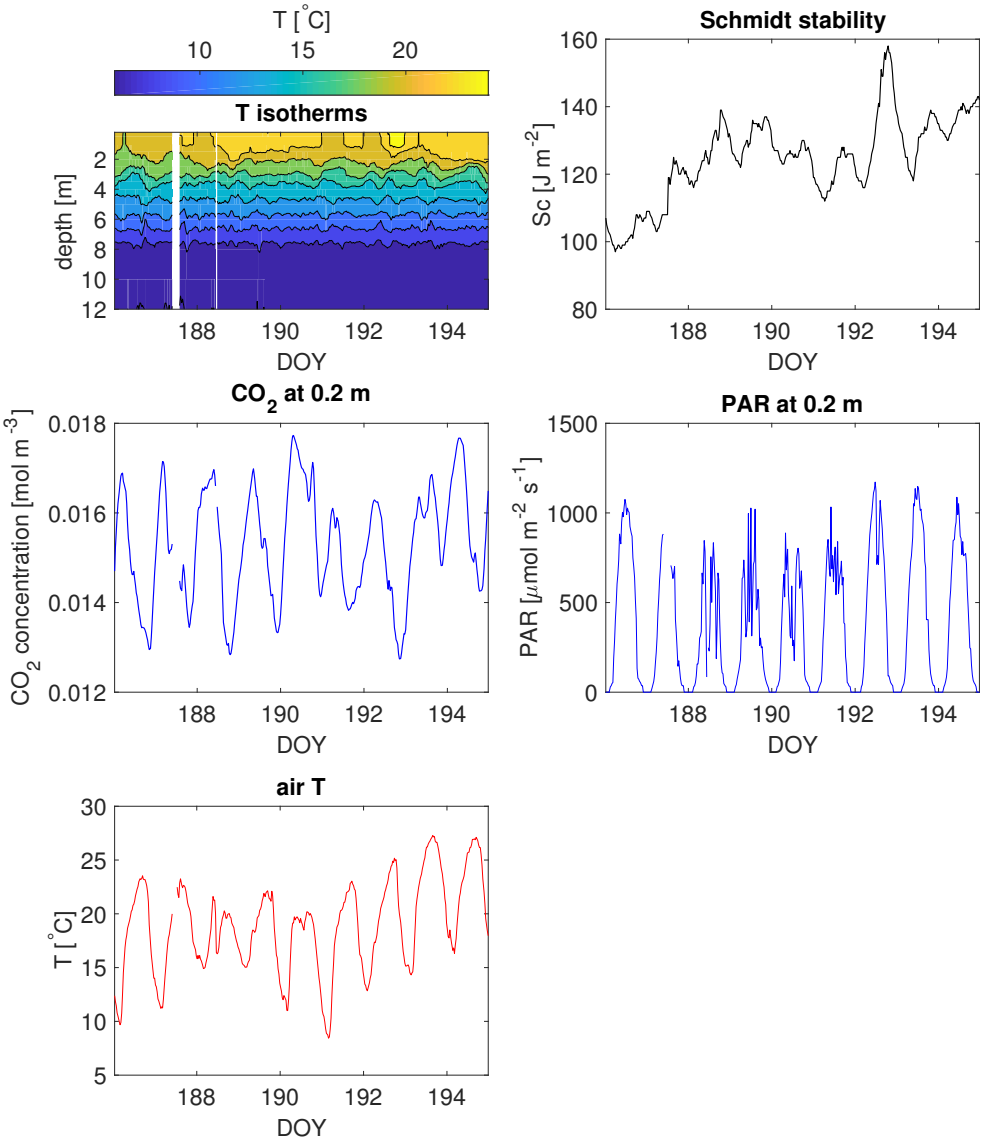

Figure S5. Time series of isotherms, Schmidt stability, CO_2 concentration and PAR at 0.2 m, and air temperature for the first period of stable stratification studied in 2010 (5 July - 13 July).

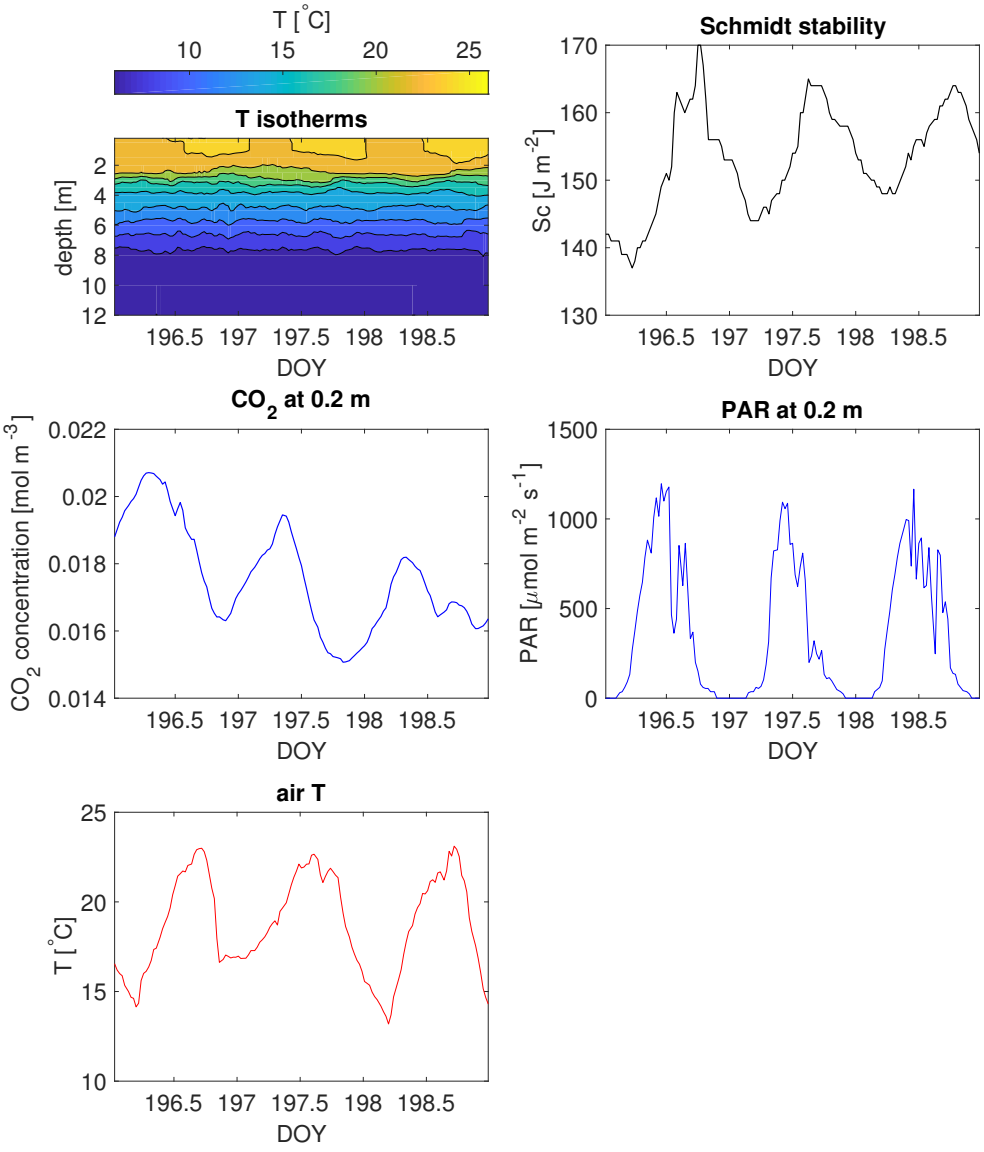

Figure S6. Time series of isotherms, Schmidt stability, CO_2 concentration and PAR at 0.2 m, and air temperature for the second period of stable stratification studied in 2010 (15 July - 17 July).

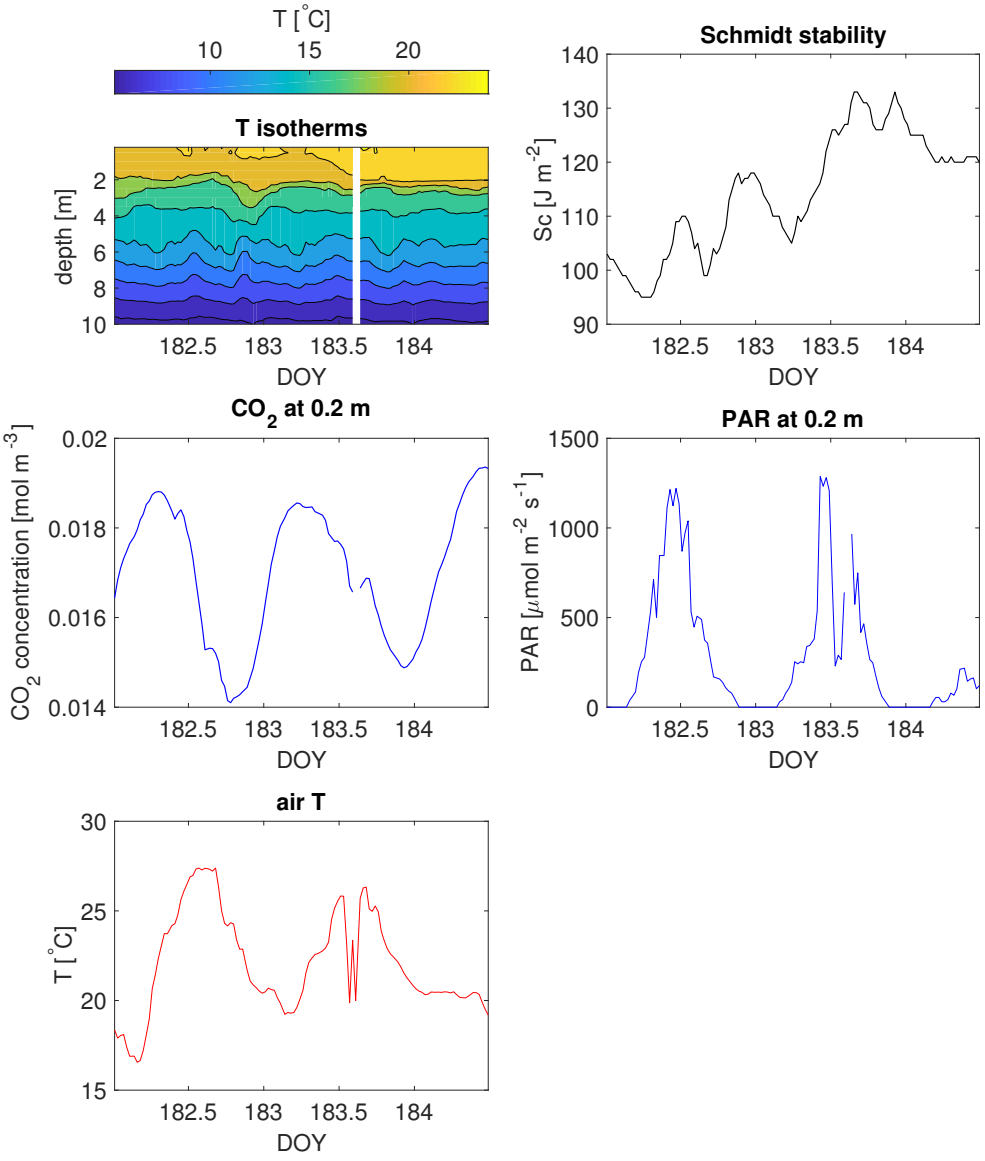

Figure S7. Time series of isotherms, Schmidt stability, CO_2 concentration and PAR at 0.2 m, and air temperature for the first period of stable stratification studied in 2011 (1 July - 3 July).

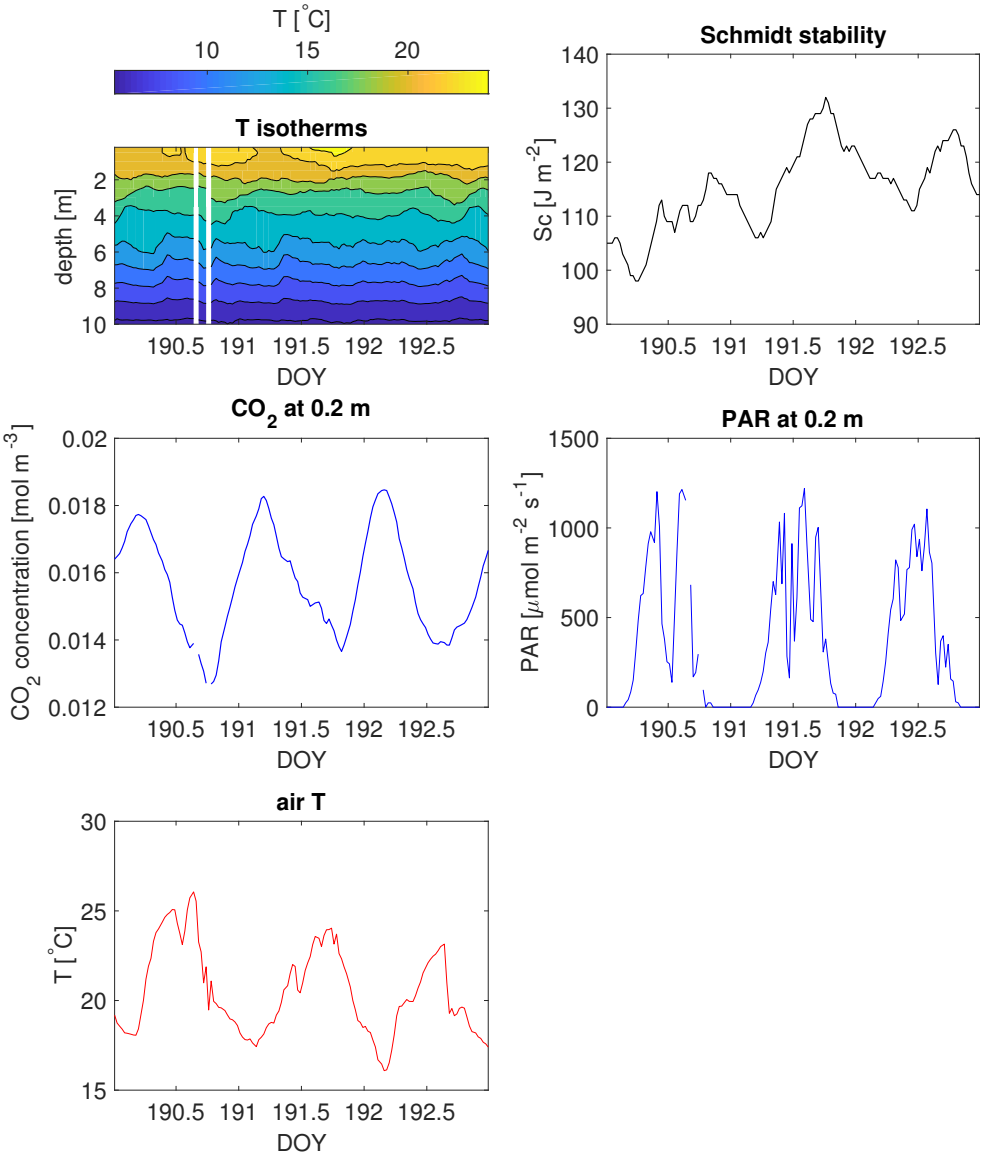

Figure S8. Time series of isotherms, Schmidt stability, CO_2 concentration and PAR at 0.2 m, and air temperature for the second period of stable stratification studied in 2011 (9 July - 11 July).

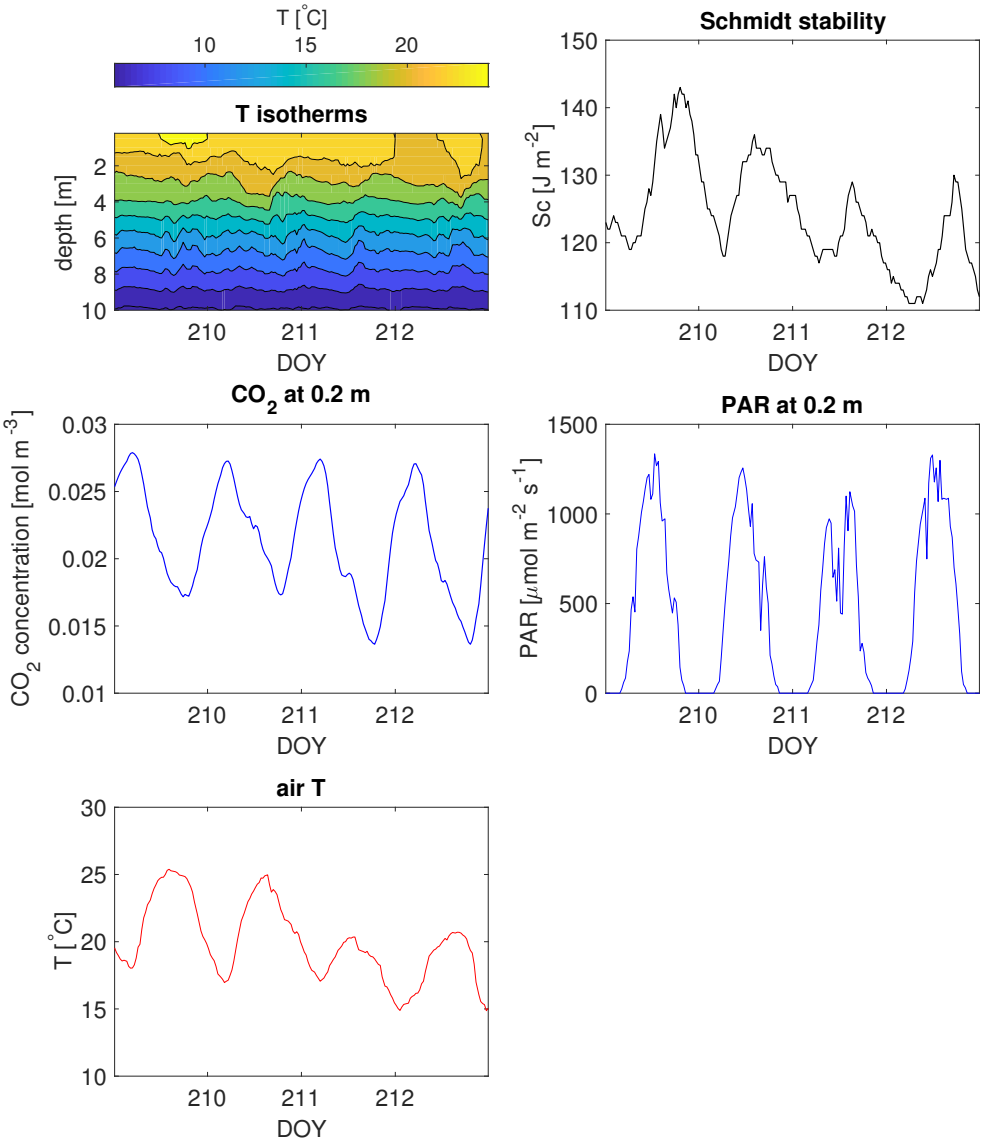

Figure S9. Time series of isotherms, Schmidt stability, CO_2 concentration and PAR at 0.2 m, and air temperature for the third period of stable stratification studied in 2011 (28 July - 31 July).

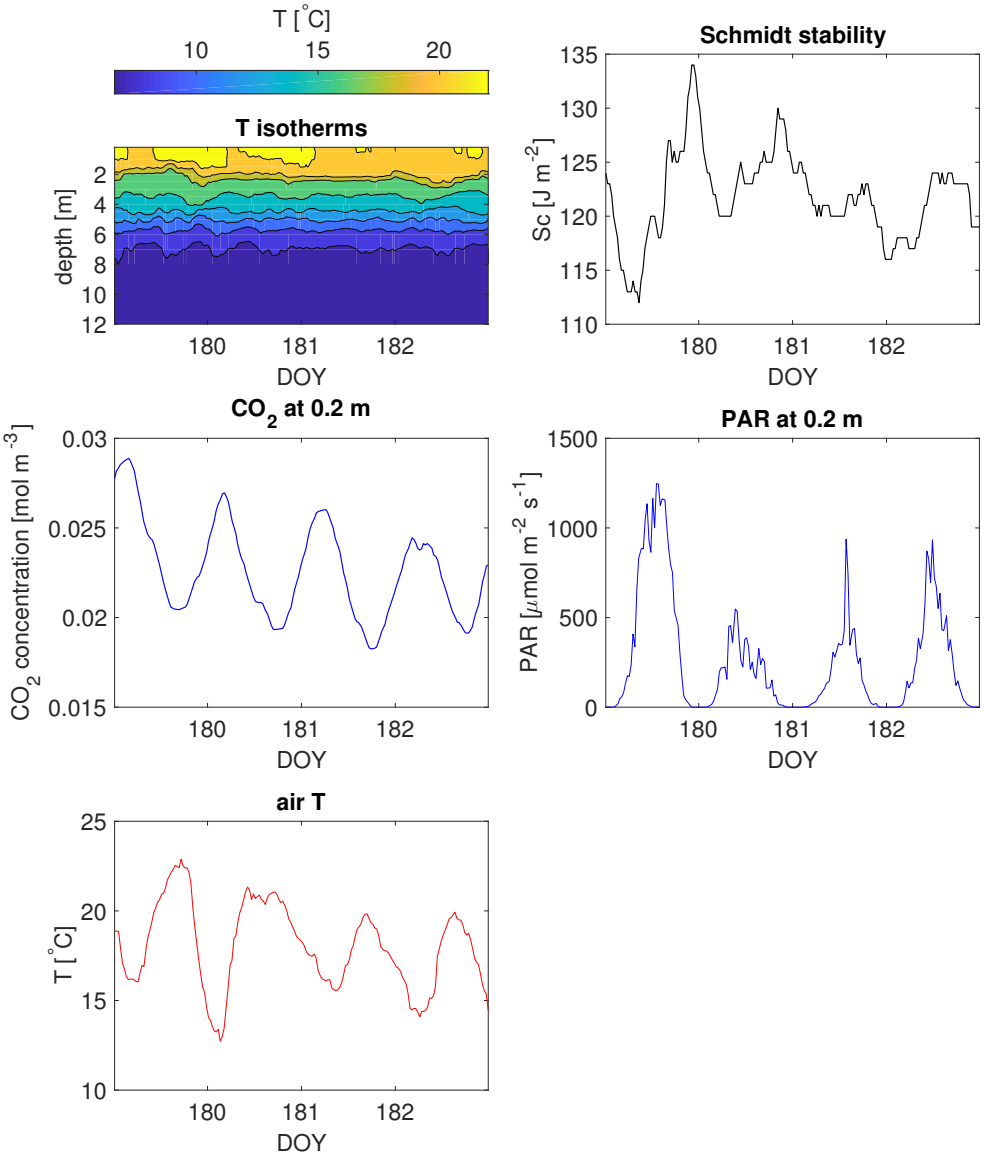

Figure S10. Time series of isotherms, Schmidt stability, CO_2 concentration and PAR at 0.2 m, and air temperature for the first period of stable stratification studied in 2013 (28 June - 1 July).

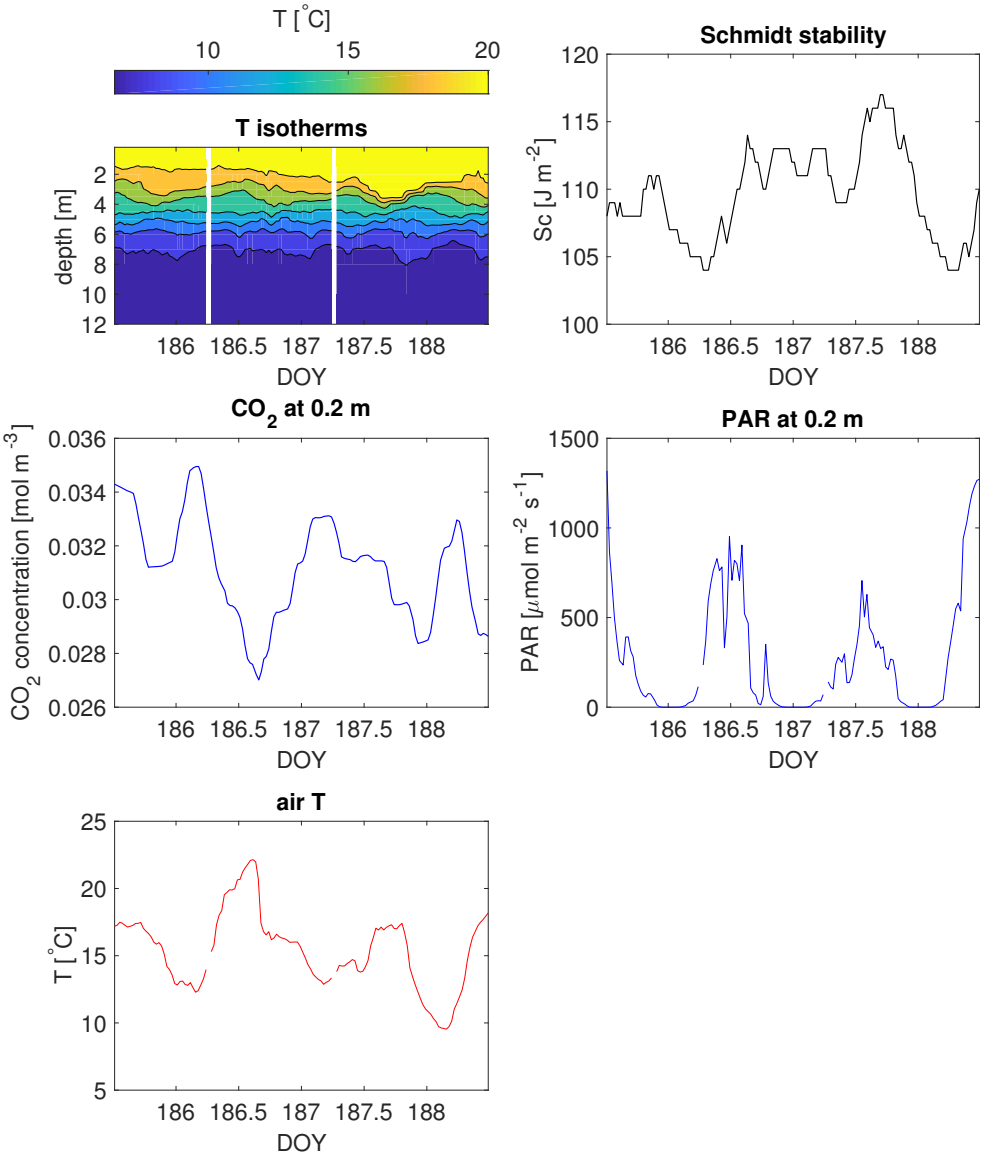

Figure S11. Time series of isotherms, Schmidt stability, CO_2 concentration and PAR at 0.2 m, and air temperature for the second period of stable stratification studied in 2013 (4 July - 7 July).

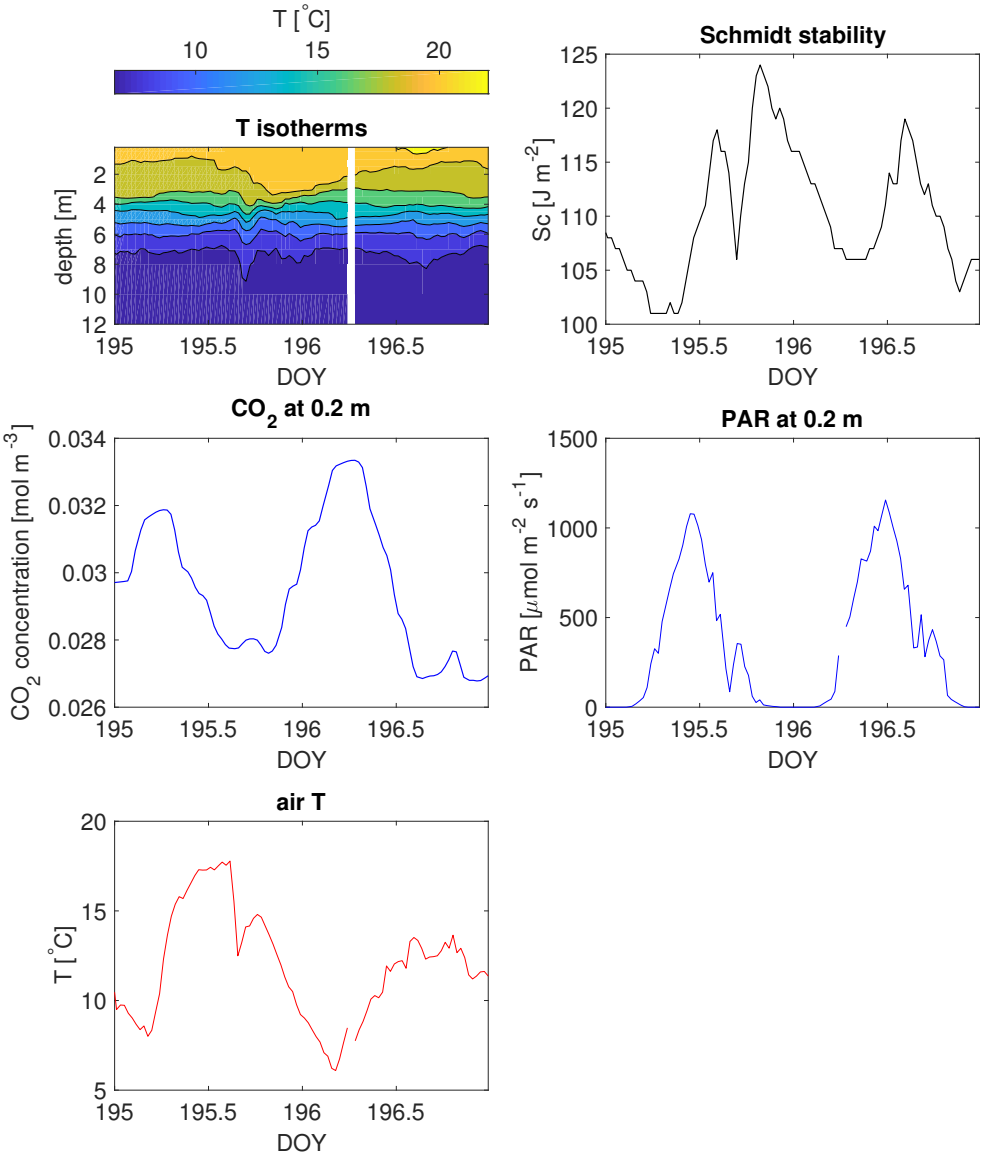

Figure S12. Time series of isotherms, Schmidt stability, CO_2 concentration and PAR at 0.2 m, and air temperature for the third period of stable stratification studied in 2013 (14 July - 15 July).

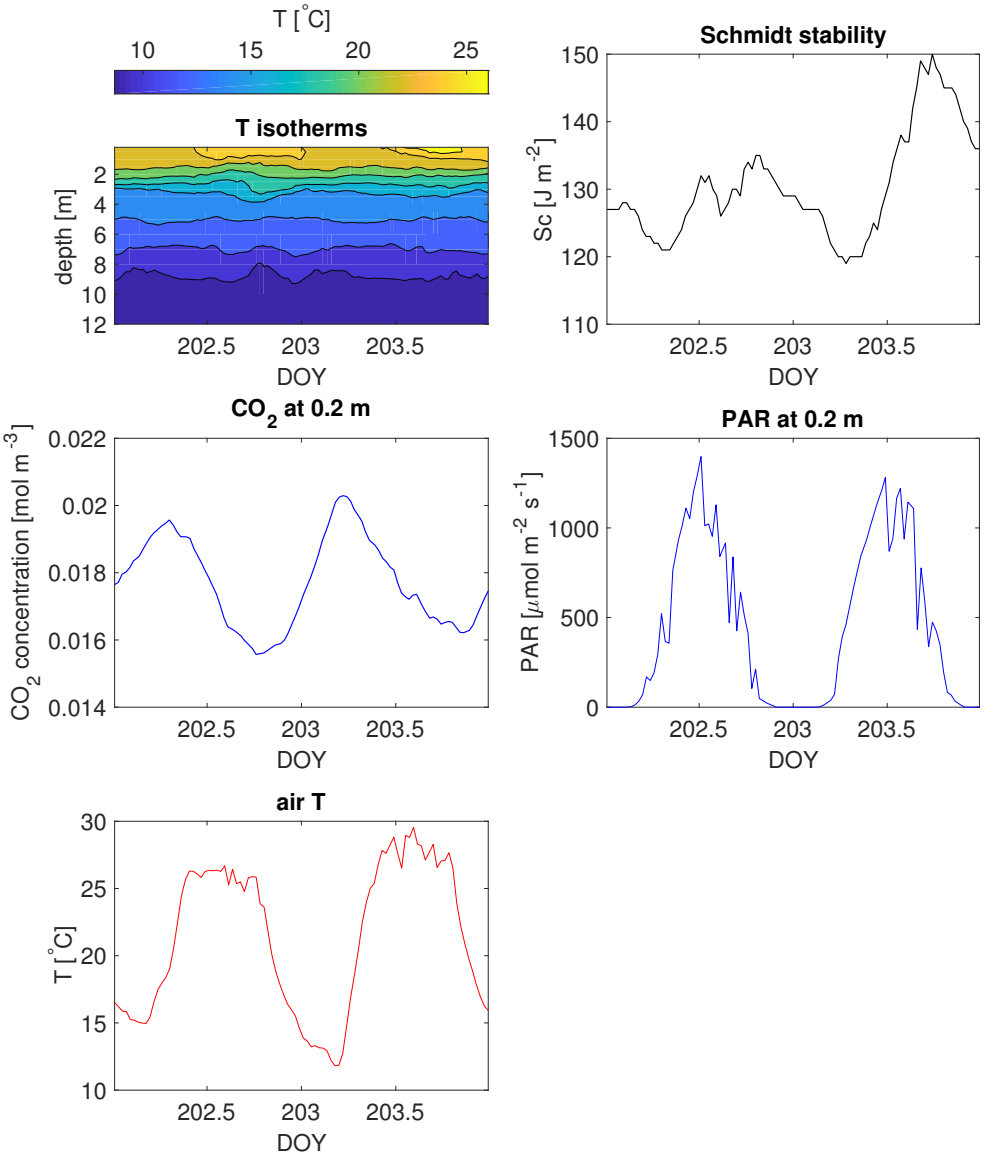

Figure S13. Time series of isotherms, Schmidt stability, CO_2 concentration and PAR at 0.2 m, and air temperature for the first period of stable stratification studied in 2014 (21 July - 22 July).

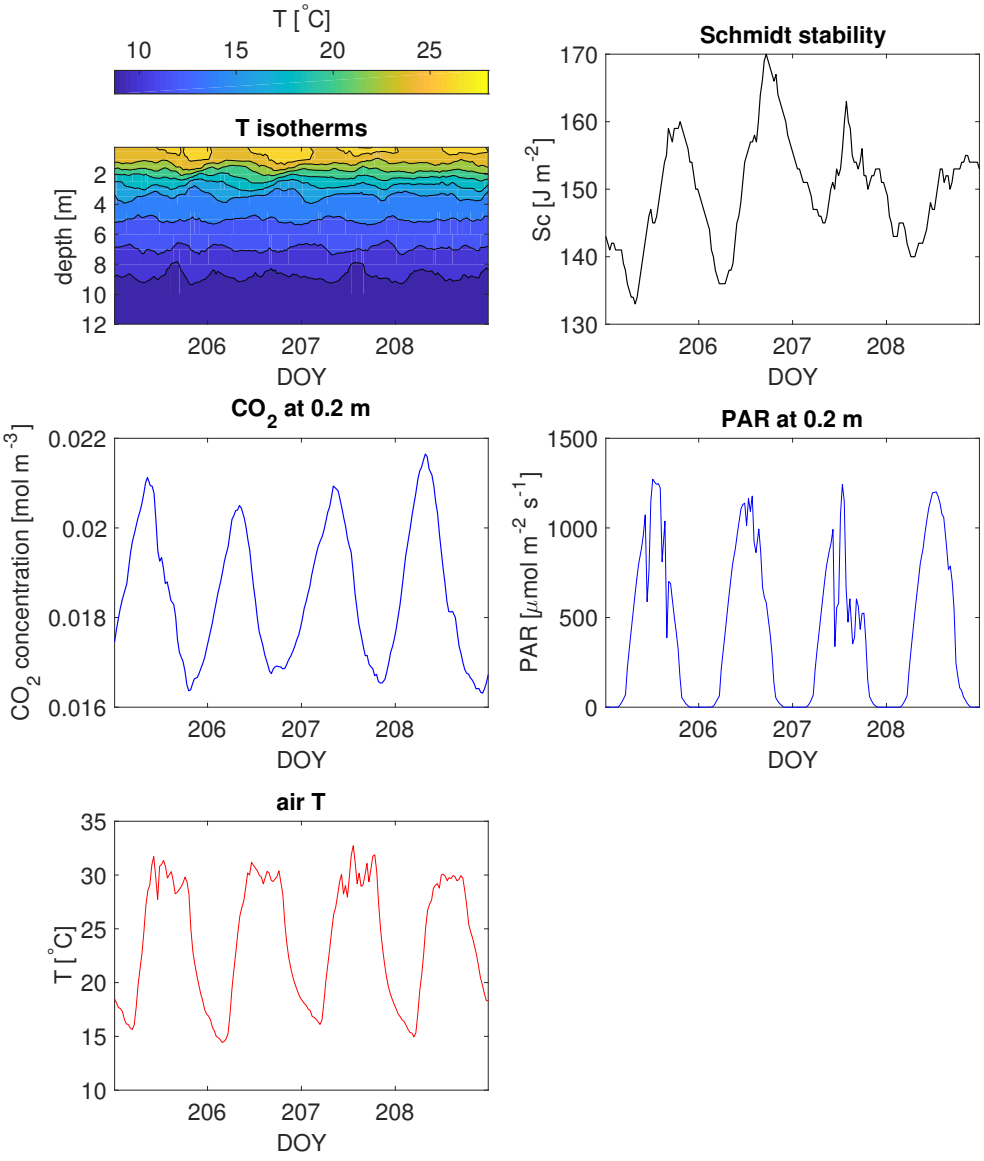

Figure S14. Time series of isotherms, Schmidt stability, CO_2 concentration and PAR at 0.2 m, and air temperature for the second period of stable stratification studied in 2014 (24 July - 27 July).

Table S1. Fit statistics (R^2 and RMSE in $\mu\mathrm{mol}(\mathrm{CO_2})\,\mathrm{m}^{-2}\,\mathrm{s}^{-1}$).

Model	2010 R^2	RMSE	2011 R^2	RMSE	2013 R^2	RMSE	2014 R^2	RMSE
Michaelis-Menten	0.73	0.23	0.84	0.25	0.71	0.14	0.74	0.33
Smith	0.76	0.22	0.85	0.25	0.70	0.15	0.74	0.33
Jassby and Platt	0.76	0.22	0.84	0.25	0.70	0.15	0.74	0.33